[Downloaded from www.aece.ro on Thursday, March 28, 2024 at 14:13:40 (UTC) by 44.220.131.93. Redistribution subject to AECE license or copyright.]

Voltage Control of Distribution Grids with Multi-Microgrids Using Reactive Power Management

Piotr WŁODARCZYK[1], Andreas SUMPER[2,3], Miguel CRUZ[2]
[1]*AGH University of Science and Technology, Department of Automatics and Biomedical Engineering, 30059, Poland*
[2]*IREC Catalonia Institute for Energy Research, 08930, Spain*
[3]*Centre d'Innovació Tecnològica en Convertidors Estàtics i Accionaments (CITCEA-UPC), Departament d'Enginyeria Elèctrica, Universitat Politècnica de Catalunya, EU d'Enginyeria Tècnica Industrial de Barcelona, 08036, Spain*
pwlodar@agh.edu.pl

***Abstract*—Low-voltage Microgrids can be valuable sources of ancillary services for the Distribution System Operators (DSOs). The aim of this paper was to study if and how multi-microgrids can contribute to Voltage Control (VC) in medium-voltage distribution grids by means of reactive power generation and/or absorption. The hierarchical control strategy was proposed with the main focus on the tertiary control which was defined as optimal power flow problem. The interior-point algorithm was applied to optimise experimental benchmark grid with the presence of Distributed Energy Resources (DERs). Moreover, two primary objectives were formulated: active power losses and amount of reactive power used to reach the voltage profile. As a result the active power losses were minimised to the high extent achieving the savings around 22% during entire day.**

***Index Terms*—distributed generation, multi-microgrids, optimal power flow, smart grids, voltage control.**

I. INTRODUCTION

The smart grid concept has gained lots of popularity in recent years as a prospect for the modernised and efficient power systems which will be able to meet the needs of the twenty-first century [1]. One of the fundamental idea encompassed by the smart grid term is the active distribution network (ADN).

In general, ADN is a distribution grid with a high penetration of Distributed Energy Resources (DERs) such as energy storage devices, wind turbines, photovoltaic panels, fuel cells etc. which make a tremendous transition from a passive, one-directional distribution system into the bidirectional one [2]. Although DERs presence in the system may have positive consequences such as smaller power losses, deregulated and competitive electricity markets or improved power quality [3] it also challenges Distribution System Operators (DSO) in terms of feeder overloads, voltage variations, power quality disturbances and incorrect protection operation [4].

Deeply studied instances of ADN with regards to management and control are low-voltage microgrids (MG), the idea firstly introduced by Lasseter in [5]. MGs can supply small communities such as residential areas, industrial sites or regional areas. They can operate in islanded and main-grid-connected mode. Moreover, from the DSO perspective MGs can be seen as either aggregated loads or power generators, and thus, they can be also a valuable source of the ancillary services such as Voltage Control (VC), congestion management, peak shaving or line balancing.

A common way of VC in power systems is the use of the reactive power resources [6]. In a typical distribution system the VC is realised by corrective devices such as tap changers and shunt capacitors. Nevertheless, many authors have studied the possibility of DERs application in VC in ADN. Richardot *et al.* [7] implement at the distribution level a hierarchical control structure reminding the one already applied in the transmission system in France [8]. The voltage is controlled by maintaining the voltage set-points at the substation and the representative buses called pilot buses. In [9] a multi-agent approach to model DERs and tap changers is applied. Agents are given two conflicting objectives to be satisfied: the reduction of the voltage variations and minimisation of control actions or maximisation of the active power coming from DERs. Furthermore, Model Predictive Control was successfully used by the researchers in [10] in order to correct the errors related to measurements and modelling inaccuracies. They addressed the need for keeping the voltage in a normal operation region along with the minimisation of the control actions.

A large number of researchers have studied the optimisation algorithms application in the VC. Agalgaonkar, Pal and Jabr optimise the collaboration of tap changers, autonomous regulators and solar power generation [11]. The decentralised optimisation approach was presented in [12] and [13]. In the former the distribution grid is divided into smaller areas which are optimised separately and only the use of DERs which influence the chosen region are optimised. In the latter, given finite data sets, the offline optimisation for the entire grid is done and the look-up tables for each inverter-based DERs are created so that they can be operated based only on the local information. There

This work was financed by KIC InnoEnergy Consortium and by the State Budget Funds assigned for statutory activity 15.11.120.421.

Digital Object Identifier 10.4316/AECE.2015.01012

1582-7445 © 2015 AECE

[Downloaded from www.aece.ro on Thursday, March 28, 2024 at 14:13:40 (UTC) by 44.220.131.93. Redistribution subject to AECE license or copyright.]

are not many papers about VC with the support of Multi-Microgrids. However, Madureira and Pecas Lopes presented interesting results in [14]. By means of evolutionary particle swarm optimisation the optimal power flow problem was solved which consisted in the minimisation of the active power losses and microgeneration shedding.

The aim of this paper was to study if and how the low-voltage microgrids can contribute to Voltage Control in medium-voltage distribution grid by means of reactive power generation and/or absorption. The paper was divided into 3 main sections. In section II the formal formulation of the problem is given along with the description of the interior-point optimisation algorithm. Section III describes the study grid, detailed control strategy and main results of the research. The paper ends up with the conclusions.

II. Problem Statement

A. Multi-Microgrid System

A Multi-Microgrid system may have a hierarchical control structure divided into tertiary, secondary and primary control which is presented in Fig. 1. Starting from the bottom, the Primary Control consists in the local control of microgeneration, energy storage and dispatchable loads. All the local controllers are governed and managed by the Microgrid controller (MGC) which is also responsible for the information exchange with the tertiary controller, in our case called the Multi-Microgrid Central Controller (MMCC). MGC is independent from the DSO and can take part in MV ancillary services. The tertiary controller, which is of our main interest in this study, coordinates the operation of the MV distribution system by the deployment of all the available resources including those offered by the MG's operators. Only voltage control via utilisation of reactive power will be discussed in this paper.

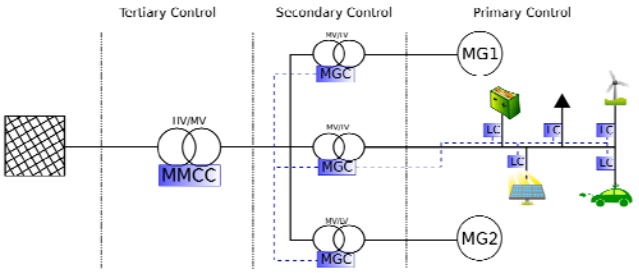


Figure 1: Hierarchical control structure of the distribution grid with Multi-Microgrids.

B. Voltage Control

Voltage control in a distribution grid can be done in various ways such as Model Predictive Control [10], Multi-agent approach [15] or can be perceived as the optimal power flow problem which consists in solving the nonlinear optimisation problem with nonlinear constraints [14]. In this paper it was decided to apply and extend the lastly-mentioned idea. It can be formally written as

$$\begin{aligned} &\min_x F(x) \\ &g_i(x) \le 0, i = 1...n \\ &h_j(x) = 0, j = 1...m \end{aligned} \tag{1}$$

where the objective function is usually expressed as a sum of active power losses in every branch of the grid [16]. However, it is reasonable to introduce a penalty coefficient for the utilisation of the reactive power in voltage control in order to limit the control actions and treat reactive power as a valuable service. The detailed formula is as follows

$$\begin{aligned} F(x) &= C_P \cdot \sum_{k=1}^{37} P_{loss} + \sum_{z=1}^{6} Q_{cost}, \\ P_{loss} &= \sum_{k=1}^{n} g_k (V_a^2 + V_b^2 - 2V_a V_b cos(\delta_a - \delta_b)) \\ Q_{cost} &= \sum_{z=1}^{6} C_{Q1} Q_{MG_z} + C_{Q2} Q_{MG_z}^2 \end{aligned} \tag{2}$$

where k is a line number between buses a and b, V_a and δ_a denote the voltage and the angle at the bus a, respectively and g_k is a k line conductance. Q_{MGz} is the reactive power at z-th microgrid bus, while C_{Q1} and C_{Q2} are Q_{cost} function coefficients. C_P is a cost of the active power. The problem is a subject to the following equality constraints for each of the a bus

$$\left.\begin{aligned} P_a(V,\delta) &= P_a^G - P_a^L \\ Q_a(V,\delta) &= Q_a^G - Q_a^L \end{aligned}\right\} \text{AC Power Flow equations} \tag{3}$$

The AC power flow equations can be formulated in various ways depending on the choice of the voltage and admittance coordinates [16-17]. In this study the formula, where the voltages are expressed in polar coordinates and the admittances takes the form of rectangular coordinates, was selected. Additionally, the inequality constraints apply

$$\begin{aligned} Q_{MG_z}^{min} &\le Q_{MG_z} \le Q_{MG_z}^{max} \\ V_a^{min} &\le V_a \le V_a^{max} \\ \delta_a^{min} &\le \delta_a \le \delta_a^{max} \end{aligned} \tag{4}$$

Voltages and angles are bounded by the DSO's voltage profile. Reactive power limits are given by a microgrid operator, reflecting the reactive power reserves at particular instant of time. Active powers at the microgrid buses, active and reactive powers at the load buses are defined in advance, they may come from the real measurements or system estimators.

The decision vector comprises voltages and angles at all of the buses apart from the slack bus at which voltage and angle equals 1 p.u. and 0, respectively (This is a consequence of the Power Flow computation assumptions [16]), reactive power at the microgrid buses and active and reactive power absorbed/generated from/to the HV grid.

$$x = [\delta \; V \; Q_M \; G_z \; P_{slack} \; Q_{slack}] \tag{5}$$

C. Optimisation Algorithm

The above-mentioned problem can be solved by means of traditional non-linear programming algorithms or by meta-heuristics such as genetic algorithms, swarm optimisation etc. The interior-point algorithm - barrier method, which is implemented in Matlab optimisation toolbox, was applied in this work. The idea of the barrier method is described in a very accessible form in [18], while the exact algorithm description is discussed in [19]. In general, the method consists in the approximation of the inequality constrained initial problem (1) by a sequence of the equality constrained subproblems in the form of

[Downloaded from www.aece.ro on Thursday, March 28, 2024 at 14:13:40 (UTC) by 44.220.131.93. Redistribution subject to AECE license or copyright.]

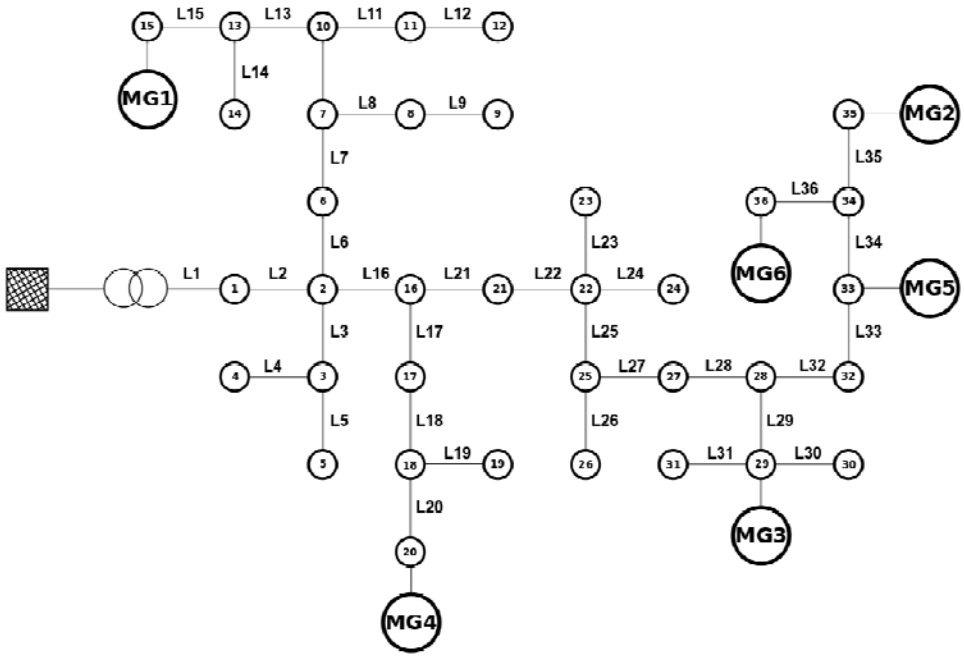


Figure 2: The IEEE 37-bus MV grid adapted to European standards with six microgrids coupled to the buses 15, 20, 29, 33, 35 and 36.

$$\begin{aligned} &\min_{x,s} F_\mu(x,s) = F(x) + \Phi(s) \\ &g_{\mu_i}(x) + s_i = 0, i = 1 \ldots m \\ &h_j(x) = 0, j = 1 \ldots n \end{aligned} \tag{6}$$

Φ(s) is a logarithmic barrier function equal to

$$\Phi(s) = -\mu \sum_{i=1}^{m} ln(s_i), \mu > 0, s_i > 0, \tag{7}$$

where s_i is a slack variable related to the *i*-th inequality constraint. By decreasing the coefficient *m* the accuracy of the approximation is increased. When it converges to 0, the minimum of F_μ equals to the minimum of the original problem (1). Each iteration is solved by the application of the SQP method with trust regions, considered efficient for the nonlinear problems with equality constraints, taking each time as a starting point the result of the former iteration. The entire algorithm is summarised below followed by [19]

Barrier Algorithm for Solving the Nonlinear Problem

Choose an initial value for the barrier parameter μ>0, and select the subproblem solution tolerance e_μ>0, $\theta \in (0,1)$ and the final stop tolerance e_{tol}. Choose the starting point x_0 and s>0, evaluate the objective function, constraints, and their derivatives at x_0. *E(x, s, m)* is an optimality measure of the solution of the barrier problem.

Repeat until $E(x_0, s, 0) \leq e_{tol}$

1. Apply an SQP method with trust regions, starting from (x_0, s) to find an approximate solution (x^*, s^*) of the barrier problem satisfying $E(x^*, s^*, \mu) \leq e_\mu$

2. Set $\mu \leftarrow \theta\mu$, $e_\mu \leftarrow \theta e_\mu$, $x_0 \leftarrow x^*$, $s \leftarrow s^*$

End

III. Study Grid

A. Grid Data

For the simulation purpose, the IEEE 37-node grid adapted to European standards coming from [20] was chosen. Grid structure with additional six microgrids coupled to the buses 15, 20, 29, 33, 35 and 36 is depicted in Fig.2. Grid parameters were specified in order to weaken the grid which resulted in low initial voltages at all buses of the system. The microgrids' placement was done arbitrarily, there were no algorithms for optimal placement used as it was out of the scope of the study. Although the initial idea was to distribute the microgrids evenly along the grid, finally most of the microgrids were located in the end of the feeder as the highest voltage variations arise over there.

The necessary grid data including nominal apparent power of all the buses, lines' and transformer's resistances and reactances are collected in Appendix A.

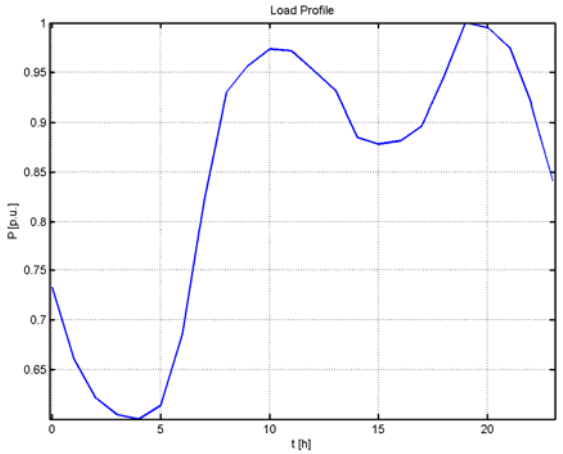


Figure 3: Normalised load profile applied to every bus in the study grid apart from the microgrid buses.

The load profile was derived from the Spanish TSO Red Electrica de España and represents Spain's daily demand for electricity during Winter and was first used in [20]. In fact, it is the normalised mean of the two-month labour-days load profiles coming from 07.01.2009 to 27.02.2009. The primary reason for the selection of Winter load profiles was the higher demand for electricity during this time of year

[Downloaded from www.aece.ro on Thursday, March 28, 2024 at 14:13:40 (UTC) by 44.220.131.93. Redistribution subject to AECE license or copyright.]

due to heating devices present in the grid. Furthermore the load profile was scaled to each bus based on their transformers' 80% nominal apparent power capacity with constant power factor which equals 0.7. Load profiles were not generated for the microgrid buses, as they can either consume or produce both active and reactive power.

Various grid scenarios realised in the microgrid emulator belonging to The Catalonia Institute for Energy Research in Barcelona (IREC)'s resulted in the microgrids' active power profiles (Fig.4), which similarly to the load profiles, were normalised and scaled to microgrid buses' transformers' 80% nominal apparent power capacity. Profile's positive value means that the power is generated from the microgrid otherwise the power is consumed.

Moreover, the power factor at which active power is generated/consumed by the microgrid equals 0.9. The IREC's microgrid technical specification can be found in [21].

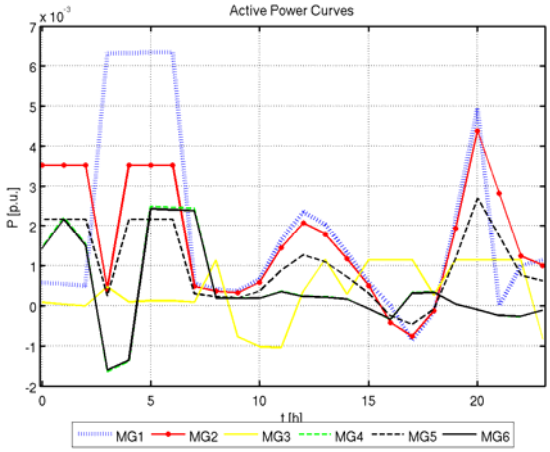


Figure 4: Microgrids' 24-hours active power profiles generated by the The Catalonia Institute for Energy Research's microgrid emulator.

B. *Control Strategy*

For the study grid described in the previous sections, the following control strategy has been proposed and applied in the experimental scenario. If for any bus in the system its voltage falls below 0.96 p.u. then the optimisation routine is run. If the optimisation algorithm does not converge to the optimum, the constraints violation is checked. If the solution is within the limits then it is accepted despite being not optimal, otherwise the solver should be tuned or changed or no action is taken. The procedure is run every hour. The control strategy is presented in the form of a block diagram in the Fig.5.

The constraints (4) were defined as follows: 0.96 p.u. $< V_i <$ 1.04 p.u., $-2\pi < \delta_i < 2\pi$, reactive power upper and lower limits were calculated as a function of the maximum available capacity of the microgrid bus transformer at a certain instant of time and the actual active power flow from/to the microgrid.

C. *Results Discussion*

The application of the above-mentioned control strategy has led to the local optimal voltage profiles at all of the buses which satisfy the constraints. In Fig. 6 one can compare and contrast the optimised voltage profiles for four representative buses 5, 9, 27, 32. They were chosen with regards to the distance from the transformer. During first 7 hours there was no need for the voltage control as all the voltages were kept over 0.96 p.u. However starting from the 8th hour the proposed algorithm was applied. Although the trend of the profiles at each of the buses is similar one can notice the slight differences in values. The voltage profiles before optimisation are in red whereas the optimised voltage profiles are in blue.

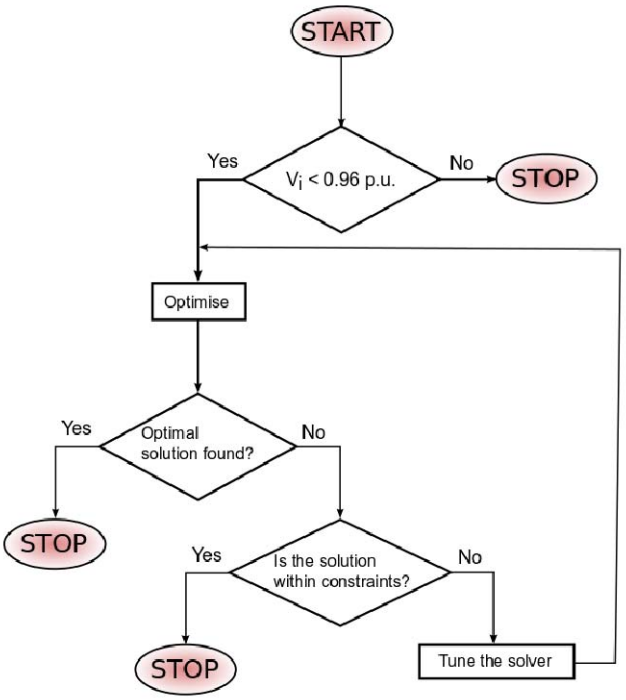


Figure 5: The block diagram of the proposed control strategy in the experimental scenario.

The optimised voltage profiles are slightly above 0.96 p.u., which is the result of the penalty function addition to the objective function i.e. only truly necessary control actions are taken in order to meet the system operator requirements. Otherwise, due to limited capacity of the microgrids, the optimal solution would always be quite predictable - the maximum of the available reactive power would be used as the optimal setpoints.

The optimised reactive power generation profiles are depicted in Fig.7. During the first seven hours Q provided/consumed by the microgrid corresponds to its active power profile by a constant inductive power factor equal to 0.9. However from 8th hour situation changes because of the optimisation routine application. What is interesting, most of the generated reactive power comes from the microgrids placed in the end of the feeder as the control actions are mostly required in that area (the reactive power influences the system locally and it cannot be transferred for long distances). During last 4/5 hours of the day MG2, MG5, MG6 are asked to provide their maximum reactive power reserves. This implies that in the given experimental grid there exists only small availability of voltage control by means of the reactive power. Instead, they can be used more as a voltage profile shaping method.

Furthermore, in Fig. 8 one can notice that when applied the optimisation routine reduces the active power losses in the grid by around 22%. The active power losses in the system with and without optimisation are 0.00215048 p.u. and 0.0027473 p.u., respectively.

[Downloaded from www.aece.ro on Thursday, March 28, 2024 at 14:13:40 (UTC) by 44.220.131.93. Redistribution subject to AECE license or copyright.]

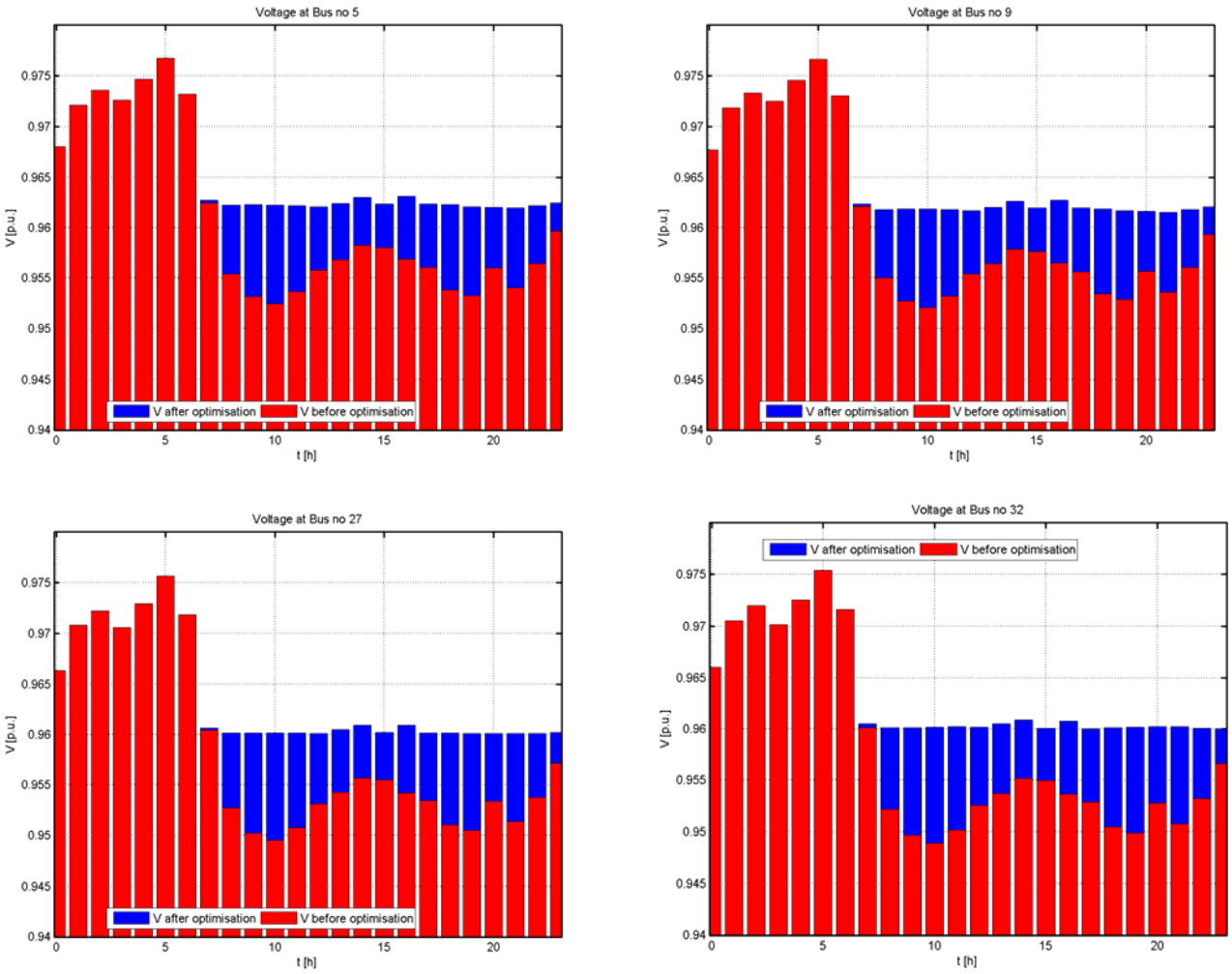


Figure 6: Voltage profiles for arbitrally chosen buses 5, 9, 27 and 32 with regards to the distance from the transformer. The results before and after optimisation are presented in blue and red, respectively.

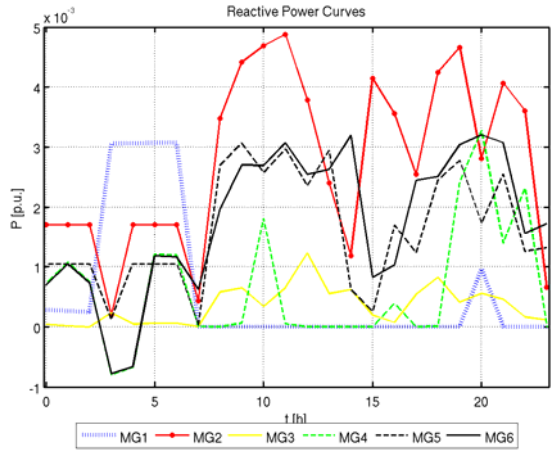


Figure 7: Microgrids' 24 hours reactive power profiles. During the first seven hours the control algorithm is not applied as the voltages at all buses in the grid are over 0.96 p.u..

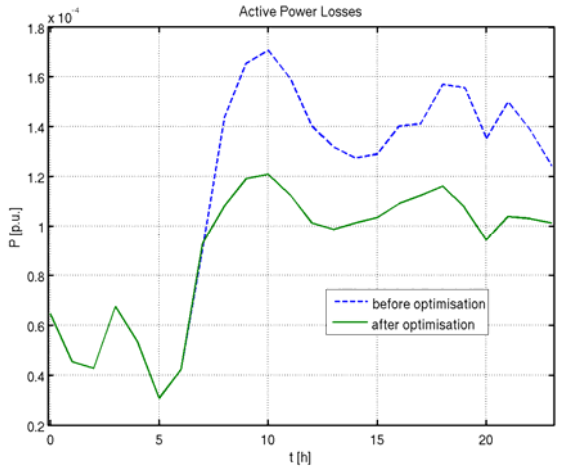


Figure 8: Active power losses before and after optimisation. During first seven hours due to no application of the optimisation routine losses for the both cases are the same.

IV. Conclusions

In this paper the MGs' contribution to voltage control by offering ancillary services such as reactive power generation was presented. First of all, the configuration proposed above where the number of MGs is small, cannot support great changes of voltage but can be used for the voltage profile shaping. Additionally, in case of too sharp conditions for the voltage profile the reactive power generation is pushed to the limits. It must be stressed that in other scenarios control strategy would be similar. However, in case of overvoltages caused by e.g. loads cut off, MGs would be used as reactive power consumers in order to decrease voltage level. Secondly, as a consequence of the application of the discussed control strategy, the active power losses were minimised to the high extent achieving the savings around 22% during entire day. In the future, more accurate microgrids' reactive power reserves estimation should be tested together with the introduction of the other voltage controllers such as tap changers, shunt capacitors etc.

[Downloaded from www.aece.ro on Thursday, March 28, 2024 at 14:13:40 (UTC) by 44.220.131.93. Redistribution subject to AECE license or copyright.]

Moreover, practical application of the algorithm would raise the value of the research if technical and financial limitations of such installation were overcome.

APPENDIX A

TABLE I. GRID DATA

Bus Number	Sn [kVA]	Line Number	R [p.u.]	Xl [p.u.]	Imax [A]	D [mm^2]
Trans.bus	25000	1	0.0037344	0.00504	530	400
1	160	2	0.0024896	0.00336	530	400
2	900	3	0.012544	0.01312	325	120
3	400	4	0.012544	0.01312	325	120
4	410	5	0.009408	0.00984	325	120
5	160	6	0.006272	0.00656	325	120
6	400	7	0.009408	0.00984	325	120
7	250	8	0.006272	0.00656	325	120
8	500	9	0.009408	0.00984	325	120
9	400	10	0.006272	0.00656	325	120
10	160	11	0.009408	0.00984	325	120
11	250	12	0.009408	0.00984	325	120
12	250	13	0.009408	0.00984	325	120
13	500	14	0.009408	0.00984	325	120
14	160	15	0.006272	0.00656	325	120
15	880	16	0.012544	0.01312	325	120
16	880	17	0.012544	0.01312	325	120
17	560	18	0.006272	0.00656	325	120
18	250	19	0.01568	0.0164	325	120
19	160	20	0.003136	0.00328	325	120
20	410	21	0.012544	0.01312	325	120
21	250	22	0.006272	0.00656	325	120
22	410	23	0.009408	0.00984	325	120
23	410	24	0.006272	0.00656	325	120
24	630	25	0.01568	0.0164	325	120
25	650	26	0.006272	0.00656	325	120
26	650	27	0.009408	0.00984	325	120
27	160	28	0.006272	0.00656	325	120
28	400	29	0.006272	0.00656	325	120
29	160	30	0.009408	0.00984	325	120
30	500	31	0.006272	0.00656	325	120
31	250	32	0.021952	0.02296	325	120
32	410	33	0.009408	0.00984	325	120
33	400	34	0.01568	0.0164	325	120
34	410	35	0.009408	0.00984	325	120
35	650	36	0.012544	0.01312	325	120
36	400	Power Base	100 MVA	Voltage Base	25 kV	

TABLE II. TRANSFORMER DATA

Transformer	R [p.u.]	Xl [p.u.]	Voltage Ratio [kV/kV]
T0	0	0.65	110/25

REFERENCES

[1] H. Farhangi, "The path of the smart grid," Power and Energy Magazine, IEEE, vol. 8, no. 1, pp. 18–28, January 2010. [Online]. Available: http:/dx.doi.org/10.1109/MPE.2009.934876

[2] S. Chowdhury and P. Crossley, "Microgrids and Active Distribution Networks," ser. IET renewable energy series. Institution of Engineering and Technology, pp. 2, 2009.

[3] J. P. Lopes, N. Hatziargyriou, J. Mutale, P. Djapic, and N. Jenkins, "Integrating distributed generation into electric power systems: A review of drivers, challenges and opportunities," Electric Power Systems Research, vol. 77, no. 9, pp. 1189 – 1203, 2007. [Online]. Available:http://dx.doi.org/10.1016/j.epsr.2006.08.016

[4] M. Bollen, "Integration of Distributed Generation in the Power System," ser. IEEE Press Series on Power Engineering. John Wiley & Sons, pp. 84-87, 2011.

[5] R. Lasseter, "Microgrids," in Power Engineering Society Winter Meeting, 2002. IEEE, vol. 1, 2002, pp. 305 – 308 [Online]. Available: http://dx.doi.org/10.1109/PESW.2002.985003

[6] P. Kundur, "Power System Stability And Control," ser. EPRI power system engineering series. McGraw-Hill Education (India) Pvt Limited, pp. 627-684, 1994.

[7] O. Richardot, Y. Besanger, D. Radu, and N. Hadjsaid, "Optimal location of pilot buses by a genetic algorithm approach for a coordinated voltage control in distribution systems," in PowerTech, 2009 IEEE Bucharest, June 2009, pp. 1–7. [Online]. Available: http://dx.doi.org/10.1109/PTC.2009.5281978

[8] J. P. Paul, J. Leost, and J.-M. Tesseron, "Survey of the secondary voltage control in France : Present realization and investigations," Power Systems, IEEE Transactions on, vol. 2, no. 2, pp. 505–511, May 1987.
[Online]. Available: http://dx.doi.org/10.1109/TPWRS.1987.4335155

[9] H. Farag and E. El-Saadany, "A novel cooperative protocol for distributed voltage control in active distribution systems," Power Systems, IEEE Transactions on, vol. 28, no. 2, pp. 1645–1656, May 2013. [Online]. Available: http://dx.doi.org/10.1109/TPWRS.2012.2221146

[10] G. Valverde and T. Van Cutsem, "Model predictive control of voltages in active distribution networks," Smart Grid, IEEE Transactions on, vol. 4, no. 4, pp. 2152–2161, Dec 2013. [Online]. Available: http://dx.doi.org/10.1109/TSG.2013.2246199

[11] Y. Agalgaonkar, B. Pal, and R. Jabr, "Distribution voltage control considering the impact of pv generation on tap changers and autonomous regulators," Power Systems, IEEE Transactions on, vol. 29, no. 1, pp. 182–192, Jan 2014. [Online]. Available: http://dx.doi.org/10.1109/TPWRS.2013.2279721

[12] L. Yu, D. Czarkowski, and F. de Leon, "Optimal distributed voltage regulation for secondary networks with dgs," Smart Grid, IEEE Transactions on, vol. 3, no. 2, pp. 959–967, June 2012. [Online]. Available: http://dx.doi.org/10.1109/TSG.2012.2190308

[13] K. Tanaka, M. Oshiro, S. Toma, A. Yona, T. Senjyu, T. Funabashi, and C.-H. Kim, "Decentralised control of voltage in distribution systems by distributed generators," Generation, Transmission Distribution, IET, vol. 4, no. 11, pp. 1251–1260, November 2010. [Online]. Available: http://dx.doi.org/10.1049/iet-gtd.2010.0003

[14] A. Madureira and J. Pecas Lopes, "Coordinated voltage support in distribution networks with distributed generation and microgrids," Renewable Power Generation, IET, vol. 3, no. 4, pp. 439–454, December 2009. [Online]. Available: http://dx.doi.org/10.1049/iet-rpg.2008.0064

[15] H. Fakham, A. Ahmidi, F. Colas, and X. Guillaud, "Multi-agent system for distributed voltage regulation of wind generators connected to distribution network," in Innovative Smart Grid Technologies Conference Europe (ISGT Europe), 2010 IEEE PES, Oct 2010, pp. 1–6. [Online]. Available: http://dx.doi.org/10.1109/ISGTEUROPE.2010.5638968

[16] S. Frank and S. Rebennack, "A primer on optimal power flow: Theory, formulation, and practical examples," Colorado School of Mines, Tech. Rep, 2012.

[17] B. Allaoua and A. Laoufi, "Optimal power flow solution using ant manners for electrical network," Advances in Electrical and Computer Engineering, vol. 9, no. 1, pp. 34–40, 2009. [Online]. Available: http://dx.doi.org/10.4316/AECE.2009.01006

[18] H. Hindi, "A tutorial on convex optimization II: duality and interior point methods," in American Control Conference, 2006, June 2006, pp. 11.
[Online]. Available: http://dx.doi.org/10.1109/ACC.2006.1655436

[19] R. H. Byrd, M. E. Hribar, and J. Nocedal, "An interior point algorithm for large scale nonlinear programming," SIAM Journal on Optimization, vol. 9, no. 4, p. 877, 1999. [Online]. Available: http://dx.doi.org/10.1137/S1052623497325107

[20] E. Valsera-Naranjo, A. Sumper, R. Villafafila-Robles, and D. Martinez-Vicente, "Probabilistic method to assess the impact of charging of electric vehicles on distribution grids," Energies, vol. 5, no. 5, pp. 1503–1531, 2012. [Online]. Available: http://dx.doi.org/10.3390/en5051503

[21] M. Marzband, A. Sumper, A. Ruiz-Alvarez, J. L. Dominguez-Garcia, and B. Tomoiaga, "Experimental evaluation of a real time energy management system for stand-alone microgrids in day-ahead markets," Applied Energy, vol. 106, no. 0, pp. 365 – 376, 2013. [Online]. Available: http://dx.doi.org/10.1016/j.apenergy.2013.02.018